1. AGENCY USE ONLY (Leave blank)	2. REPORT DATE	3. REPORT TYPE AND DATES COVERED
	SEPTEMBER 1993	FINAL

4. TITLE AND SUBTITLE
An Analytical Evaluation of Turbulence-induced Flexural Noise in Planar Arrays of Extended Sensors

5. FUNDING NUMBERS
PE - 63504N
TA - S0223
WU - DN780-137

6. AUTHOR(S)
Robert E. Montgomery and Bertrand Dubus

7. PERFORMING ORGANIZATION NAME(S) AND ADDRESS(ES)
NAVAL RESEARCH LABORATORY
UNDERWATER SOUND REFERENCE DETACHMENT
PO BOX 568337
ORLANDO, FL 32856-8337

8. PERFORMING ORGANIZATION REPORT NUMBER

9. SPONSORING/MONITORING AGENCY NAME(S) AND ADDRESS(ES)
COMMANDER
NAVAL SEA SYSTEMS COMMAND
WASHINGTON, DC 20362-5101

10. SPONSORING/MONITORING AGENCY REPORT NUMBER

11. SUPPLEMENTARY NOTES

12a. DISTRIBUTION/AVAILABILITY STATEMENT
Approved for public release; distribution unlimited.

12b. DISTRIBUTION CODE

13. ABSTRACT *(Maximum 200 words)*

Large-area, hull-mounted conformal sonar arrays typically employ extended sensors that are configured to detect acoustic signals by means of thickness strains that are induced by the incident pressure field. In most cases, extended sensors also have an appreciable sensitivity to strains in the lateral dimensions. Thus flexure of such a sensor would induce a signal that would not be differentiated from that of a target. Hull-mounted conformal arrays are evolving toward using lightweight, flexible sensors and support structures; therefore, flexure-induced noise is an ever present concern. This paper presents an analytical approach and a general mathematical model for the noise arising from flexure of the array support plate coupled into the array via the lateral sensitivity of the sensor. The excitation that drives the flexure is assumed to be the turbulent boundary layer created by motion of the platform through the external fluid medium. An analytical expression is derived for the equivalent plane-wave spectral density for this noise source. The result is expressed in terms of the frequency response function of the plate, the wave-number-frequency spectral density of the excitation, and the spatial filtering characteristics of the array.

14. SUBJECT TERMS		15. NUMBER OF PAGES
FLow noise	Sonar	12
Planar arrays	Flexural noise	16. PRICE CODE
Extended sensors	Power spectrum	

17. SECURITY CLASSIFICATION OF REPORT	18. SECURITY CLASSIFICATION OF THIS PAGE	19. SECURITY CLASSIFICATION OF ABSTRACT	20. LIMITATION OF ABSTRACT
UNCLASSIFIED	UNCLASSIFIED	UNCLASSIFIED	UL

GENERAL INSTRUCTIONS FOR COMPLETING SF 298

The Report Documentation Page (RDP) is used in announcing and cataloging reports. It is important that this information be consistent with the rest of the report, particularly the cover and title page. Instructions for filling in each block of the form follow. It is important to ***stay within the lines*** to meet ***optical scanning requirements***.

Block 1. Agency Use Only *(Leave blank)*.

Block 2. Report Date. Full publication date including day, month, and year, if available (e.g. 1 Jan 88). Must cite at least the year.

Block 3. Type of Report and Dates Covered. State whether report is interim, final, etc. If applicable, enter inclusive report dates (e.g. 10 Jun 87 - 30 Jun 88).

Block 4. Title and Subtitle. A title is taken from the part of the report that provides the most meaningful and complete information. When a report is prepared in more than one volume, repeat the primary title, add volume number, and include subtitle for the specific volume. On classified documents enter the title classification in parentheses.

Block 5. Funding Numbers. To include contract and grant numbers; may include program element number(s), project number(s), task number(s), and work unit number(s). Use the following labels:

C	- Contract	**PR**	- Project
G	- Grant	**TA**	- Task
PE	- Program Element	**WU**	- Work Unit Accession No.

Block 6. Author(s). Name(s) of person(s) responsible for writing the report, performing the research, or credited with the content of the report. If editor or compiler, this should follow the name(s).

Block 7. Performing Organization Name(s) and Address(es). Self-explanatory.

Block 8. Performing Organization Report Number. Enter the unique alphanumeric report number(s) assigned by the organization performing the report.

Block 9. Sponsoring/Monitoring Agency Name(s) and Address(es). Self-explanatory.

Block 10. Sponsoring/Monitoring Agency Report Number. *(If known)*

Block 11. Supplementary Notes. Enter information not included elsewhere such as: Prepared in cooperation with...; Trans. of...; To be published in.... When a report is revised, include a statement whether the new report supersedes or supplements the older report.

Block 12a. Distribution/Availability Statement. Denotes public availability or limitations. Cite any availability to the public. Enter additional limitations or special markings in all capitals (e.g. NOFORN, REL, ITAR).

- **DOD** - See DoDD 5230.24, "Distribution Statements on Technical Documents."
- **DOE** - See authorities.
- **NASA** - See Handbook NHB 2200.2.
- **NTIS** - Leave blank.

Block 12b. Distribution Code.

- **DOD** - Leave blank.
- **DOE** - Enter DOE distribution categories from the Standard Distribution for Unclassified Scientific and Technical Reports.
- **NASA** - Leave blank.
- **NTIS** - Leave blank.

Block 13. Abstract. Include a brief *(Maximum 200 words)* factual summary of the most significant information contained in the report.

Block 14. Subject Terms. Keywords or phrases identifying major subjects in the report.

Block 15. Number of Pages. Enter the total number of pages.

Block 16. Price Code. Enter appropriate price code *(NTIS only)*.

Blocks 17. - 19. Security Classifications Self-explanatory. Enter U.S. Security Classification in accordance with U.S. Security Regulations (i.e., UNCLASSIFIED). If form contains classified information, stamp classification on the top and bottom of the page.

Block 20. Limitation of Abstract. This block must be completed to assign a limitation to the abstract. Enter either UL (unlimited) or SAR (same as report). An entry in this block is necessary if the abstract is to be limited. If blank, the abstract is assumed to be unlimited.

An analytical evaluation of turbulence-induced flexural noise in planar arrays of extended sensors

Robert E. Montgomery
Naval Research Laboratory, Underwater Sound Reference Detachment, P.O. Box 568337, Orlando, Florida 32856-8337

Bertrand Dubus
Institut Superieur d'Electronique du Nord, 41 Boulevard Vauban, 59046 Lille Cedex, France

(Received 15 October 1992; revised 1 March 1993; accepted 15 May 1993)

Large-area, hull-mounted conformal sonar arrays typically employ extended sensors that are configured to detect acoustic signals by means of thickness strains that are induced by the incident pressure field. In most cases, extended sensors also have an appreciable sensitivity to strains in the lateral dimensions. Thus flexure of such a sensor would induce a signal that would not be differentiated from that of a target. Hull-mounted conformal arrays are evolving toward using lightweight, flexible sensors and support structures; therefore, flexure-induced noise is an ever present concern. This paper presents an analytical approach and a general mathematical model for the noise arising from flexure of the array support plate coupled into the array via the lateral sensitivity of the sensor. The excitation that drives the flexure is assumed to be the turbulent boundary layer created by motion of the platform through the external fluid medium. An analytical expression is derived for the equivalent plane-wave spectral density for this noise source. The result is expressed in terms of the frequency response function of the plate, the wave-number-frequency spectral density of the excitation, and the spatial filtering characteristics of the array. An application is discussed to show that predictions can be obtained in closed form.

PACS numbers: 43.20.Tb, 43.30.Lz, 43.40.Qi, 43.88.Hz

INTRODUCTION

Large-area conformal arrays that can be mounted to the hull of a ship offer unique tactical advantages over towed arrays. The performance of such arrays is usually limited by self-noise and platform noise. In the latter category, the noise induced by the turbulent boundary layer, located near the hull, is a major concern.

Boundary layer turbulence produces a random pressure field that will be detected by the array as a noise source. This is the so-called direct path for flow noise. This path for flow noise exists more or less independently of how the sensors are supported and whether or not they are point sensors versus extended sensors. Flow noise degrades the signal-to-noise ratio but can be reduced by using outer decoupler blankets that serve to attenuate the turbulent boundary layer (TBL) pressure field. The use of extended sensors to provide spatial filtering of the flow noise is also an attractive way to diminish flow noise.

Secondary sources for flow-induced noise can also be significant. If the structural support plate (SSP) is relatively lightweight and compliant, then the TBL can induce flexure of the SSP, which then serves as a secondary source of noise. This noise can enter the array via direct flexure of the extended sensors or as acoustic noise radiated by the SSP. The radiated component has been addressed by other investigators.[1-8] The former source, flexure induced into the sensors, is the focus of this paper.

The problem will be modeled as follows: the SSP, sensor array, and outer decoupler (OD) are considered to constitute a curved, layered shell with water on the OD side and a vacuum on the SSP side. A vacuum backing was chosen because it is simple to model and, in addition, it represents a worst-case scenario; i.e., the case in which the SSP is backed by a pressure-release baffle. The Corcos[9] model will be used for the TBL pressure spectrum although the theoretical development is quite applicable for any model of the wall pressure spectral density. This baseline model is illustrated in Fig. 1. The formalism to be developed makes no presumptions about the boundary conditions on the plate. Later we shall assume that the edges are simply supported in order to illustrate a specific application. Numerous analytical studies of shell and plate motion indicate that simple supports, for a large shell or plate, usually give results that accurately reflect the actual response of a plate supported in more complicated ways. The fluid loading on the plate will be included by using a rather simple model developed by Junger and Feit.[10] The validity of this model will be established by comparing the in-water displacements so derived with the more exact predictions of Sandman's model.[11]

I. ARRAY RESPONSE TO PLATE FLEXURE

Typically, the extended sensor array is situated on or very near the SSP as shown in Fig. 2. The sensors will be strained laterally if the plate flexes in response to an external excitation; therefore, noise will be generated if the sensor possesses lateral sensitivity. The TBL excitation will also be detected by the array, even if the plate is rigid; this is the so-called direct path for flow noise as discussed ear-

 0001-4966/93/94(3)/1688/12/$6.00

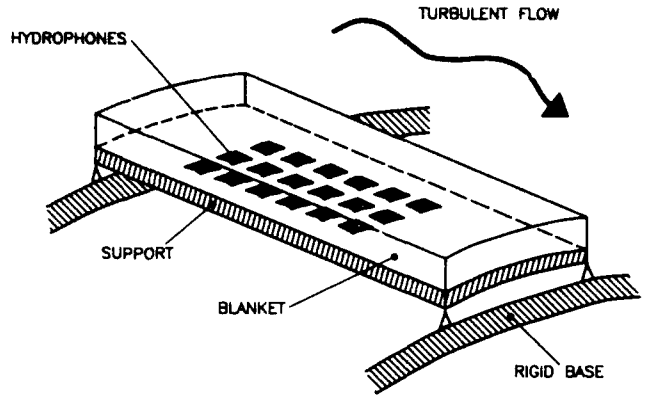

FIG. 1. Configuration of baseline problem.

lier. In order to analyze only the flexural contribution, it will be assumed that the sensors do not respond to the direct component.

The flexural response of a piezoelectric plate has been modeled by Ricketts.[12] The relevant constitutive equations are

$$T_1 = C_{11}^D S_1 + C_{12}^D S_2 - h_{31} D_3, \tag{1a}$$

$$T_2 = C_{12}^D S_1 + C_{22}^D S_2 - h_{32} D_3, \tag{1b}$$

$$E_3 = -h_{31} S_1 - h_{32} S_2 + \beta_{33}^S D_3, \tag{1c}$$

and

$$T_3 = T_4 = T_5 = 0, \tag{1d}$$

where T, S, E, and D represent stress, strain, electric field intensity, and electric displacement, respectively. The matrix components C_{ij}^D, β_{33}^s, and h_{ij} are the elastic, dielectric, and piezoelectric material constants.[13] The superscripts indicate that the designated parameters are held constant.

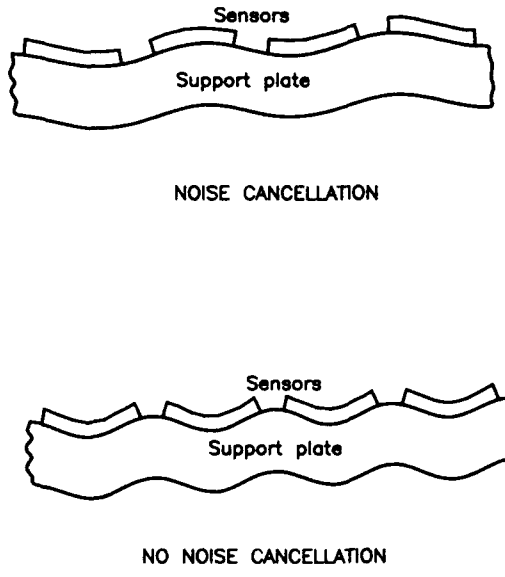

FIG. 2. Mechanism by which flexural noise can be induced via the lateral response of the sensors.

According to thin-plate theory, the strains S_1 and S_2 are related to w, the displacement of the plate, as follows:

$$S_1 = -d\frac{\partial^2 w}{\partial x^2} \quad \text{and} \quad S_2 = -d\frac{\partial^2 w}{\partial y^2}, \tag{2}$$

where d is the distance from the sensor midplane to the neutral plane. Here, S_1 and S_2 are assumed to be constant through the thickness of the sensor, and D_3 is also constant through the thickness, as can be shown by applying Gauss' law to a dielectric. Consequently, E_3 is constant through the thickness and we can write

$$E_3 = V/a, \tag{3}$$

where V is the voltage between the electrodes and a is the thickness of the sensor.

Assume that the hydrophones are electrically connected in parallel, which is equivalent to steering the array to broadside. Typically, piezoelectric sensors operate in an open circuit mode; hence, the total charge Q_T appearing on the electrodes is zero. Therefore, since D_3 corresponds to the charge density, we can write

$$Q_T = 0 = \sum_{i=1}^{N} \int_{x_i}^{x_i'} \int_{y_i}^{y_i'} D_3 \, dx \, dy, \tag{4}$$

where the integrals are performed over the lateral dimensions of each sensor. Here, N denotes the total number of sensors in the array. Using Eq. (1c), we obtain

$$\sum_{i=1}^{N} \int_{x_i}^{x_i'} \int_{y_i}^{y_i'} \left(\frac{V}{a} + h_{31} S_1 + h_{32} S_2\right) dx \, dy = 0. \tag{5}$$

The first term is independent of x and y; therefore,

$$\sum_{i=1}^{N} \int_{x_i}^{x_i'} \int_{y_i}^{y_i'} \frac{V}{a} \, dx \, dy = \frac{N l_x l_y}{a} V, \tag{6}$$

where l_x and l_y are the lateral dimensions of an individual sensor. Combining Eq. (5) with Eq. (6) we can write

$$V = \frac{a}{N l_x l_y} \int_{-\infty}^{\infty} \int (h_{31} S_1 + h_{32} S_2) A(x,y) \, dx \, dy, \tag{7}$$

where $A(x,y)$ is an array sensitivity function defined in such a way as to turn the summation into a continuous integration. For an unshaded array of unshaded hydrophones we can write

$$A(x,y) = \begin{cases} 1, & \text{if } (x,y) \text{ is on a sensor,} \\ 0, & \text{if } (x,y) \text{ is not on a sensor.} \end{cases} \tag{8}$$

Equation (7) gives the flexural noise response (in volts) in terms of the strain components S_1 and S_2. If the external excitation function is deterministic, then there will exist unique, well-defined strains that can be computed with thin plate or shell theories. On the other hand, if the excitation is a random pressure field (such as TBL), then the displacement and strains must be thought of as stochastic variables, which can be represented by a probability distribution function. In such cases, the voltage induced into the array will also be a distributed variable. Therefore,

in order to properly assess the noise due to flexure, one must account for the statistical nature of the excitation, which in our case is the turbulent boundary layer.

Before proceeding with the development of a stochastic model, it is convenient to express the noise sensed by the array in terms of an equivalent-plane-wave pressure field. This will allow direct comparison of flexural noise with ambient sea noise and other noise specifications. In a free-field environment the sensors operate in a hydrostatic mode. An incoming plane wave of amplitude P will produce an electric field E_3 across the electrodes of a nonflexing sensor of magnitude

$$E_3=(g_{33}+g_{31}+g_{32})P, \tag{9}$$

where g_{33} is the transverse piezoelectric constant, and g_{31} and g_{32} are the lateral piezoelectric constants for a piezoelectric slab that is poled through its thickness. Since E_3 is constant through the thickness, the voltage across the electrodes is $V=E_3a$. Therefore,

$$V=(ag_h)P, \tag{10}$$

where $g_h=g_{33}+g_{31}+g_{32}$ is known as the hydrostatic g constant. Equation (10) allows Eq. (7) to be expressed in terms of an equivalent-plane-wave pressure field impinging on an array in the free field.

II. POWER SPECTRAL DENSITY FOR FLEXURAL NOISE

The spectral density $\Phi_{pp}(\omega)$ for direct flow noise is typically computed by the following relationship:

$$\Phi_{pp}(\omega)=\int\int d^2k\, A(\mathbf{k},\mathbf{k}_s,\omega)H(\mathbf{k},\omega)T(\mathbf{k},\omega)P(\mathbf{k},\omega), \tag{11}$$

where $A(\mathbf{k},\mathbf{k}_s,\omega)$ is the array function steered to $\mathbf{k}_s$, $H(\mathbf{k},\omega)$ is the hydrophone function, $T(\mathbf{k},\omega)$ is the transfer function, and $P(\mathbf{k},\omega)$ is the wall pressure spectrum. The essential features of the derivation of this relationship are established in references.[14–17] Equation (11) expresses the direct TBL noise level at the sensor, but it does not account for flexurally induced noise that couples to the lateral sensitivity. Therefore Eq. (11) is not appropriate for the problem under consideration. Starting with the first principles that govern random vibration theory, an analogous expression for flexural noise can be derived. The result will be formally similar to Eq. (11), but the interpretation of the component functions will be quite different.

III. DERIVATION OF THE POWER SPECTRAL DENSITY FOR FLEXURAL NOISE

The following derivation of the power spectral density employs the notation and terminology found in *Probabilistic Theory of Structural Dynamics* by Lin.[18]

By combining Eqs. (7) and (10) we can express the equivalent pressure as

$$P(t)=\frac{1}{Ng_hl_xl_y}\int_{-\infty}^{\infty}\int(h_{31}S_1+h_{32}S_2)\,dx\,dy. \tag{12}$$

As indicated previously, the excitation field is random; therefore, the array output voltage, and hence the equivalent-plane-wave pressure, must be considered as random variables. The transverse displacement w and the lateral strains S_1 and S_2 are also random variables. The power spectral density for the equivalent-plane-wave pressure can be found by taking the Fourier transform of the corresponding correlation function $R_{pp}(t,t')$ that is defined as

$$R_{pp}(t,t')=E[P(t)P(t')], \tag{13}$$

where $E[\,]$ indicates the expected value. Because P depends linearly on S_1 and S_2, we obtain from Eq. (12)

$$\begin{aligned}R_{pp}(t,t')=\left(\frac{1}{Ng_hl_xl_y}\right)^2\int_{-\infty}^{\infty}\int d^2\mathbf{r}\int_{-\infty}^{\infty}\int d^2\mathbf{r}'[&h_{31}^2R_{S_1S_1}(\mathbf{r},t,\mathbf{r}',t')\\&+2h_{31}h_{32}R_{S_1S_2}(\mathbf{r},t,\mathbf{r}',t')\\&+h_{32}^2R_{S_2S_2}(\mathbf{r},t,\mathbf{r}',t')]A(\mathbf{r})A(\mathbf{r}'),\end{aligned} \tag{14}$$

where $R_{S_1S_1}$, $R_{S_1S_2}$, and $R_{S_2S_2}$ are the cross correlations on strains. For example,

$$R_{S_1S_2}(\mathbf{r},t,\mathbf{r}',t')=E[S_1(\mathbf{r},t)S_2(\mathbf{r}',t')]. \tag{15}$$

Let $h(\mathbf{r},\mathbf{r}',t,t')$ denote the impulse response function of the plate, which is defined as the displacement of the plate at $\mathbf{r},t$ due to an impulsive load given by

$$P_I(r,t)=\delta(\mathbf{r}-\mathbf{r}')\delta(t-t'), \tag{16}$$

that is applied at $\mathbf{r}',t'$. The principle of causality requires that $h(\mathbf{r},\mathbf{r}',t,t')$ be zero when $t<t'$. A general excitation can be represented by a superposition of impulses; likewise, the displacement can be represented as a superposition of impulse responses when the system is linear. In addition, h will depend only on the difference $t-t'$. Thus we can write

$$w(\mathbf{r},\mathbf{t})=\int_0^t d\tau\int\int_R d^2\mathbf{r}'\,h(\mathbf{r},\mathbf{r}',t-\tau)P(\mathbf{r}',\tau), \tag{17}$$

where P is the applied pressure and R is the region occupied by the plate.

The in-plane strains are, therefore,

$$\begin{aligned}S_1(\mathbf{r},t)&=-d\frac{\partial^2w}{\partial x^2}\\&=-d\int_0^t d\tau\int\int_R d^2r'\,h_{xx}(\mathbf{r},\mathbf{r}',t-\tau)P(\mathbf{r}',\tau)\end{aligned} \tag{18}$$

and

$$S_2(\mathbf{r},t) = -d\frac{\partial^2 w}{\partial y^2}$$

$$= -d\int_0^t d\tau \iint_R d^2r'\, h_{yy}(\mathbf{r},\mathbf{r}',t-\tau)P(\mathbf{r}',\tau), \tag{19}$$

where $h_{xx}=\partial^2 h/\partial x^2$ and $h_{yy}=\partial^2 h/\partial y^2$.

Using Eqs. (18) and (19), the correlation functions for strains can be written as[18]

$$R_{S_1S_1}(\mathbf{r},t,\mathbf{r}',t')$$

$$= d^2\int_0^t d\tau \int_0^{t'} d\tau' \iint_R d^2s \iint_R d^2s'\, h_{xx}(\mathbf{r},\mathbf{s},t-\tau)$$

$$\times h_{xx}(\mathbf{r}',\mathbf{s}',t'-\tau')R_{pp}(\mathbf{s},\tau;\mathbf{s}',\tau'), \tag{20}$$

where R_{pp} is the correlation on pressure. Similar expressions are found for $R_{S_1S_2}$ and $R_{S_2S_2}$. The cross spectral densities are obtained from the Fourier transforms of the correlation functions. For example, the cross spectral density for S_1 is given by

$$\Phi_{S_1S_1}(\mathbf{r},\omega,\mathbf{r}',\omega') = \left(\frac{1}{2\pi}\right)^2 \int_{-\infty}^{\infty}\int_{-\infty}^{\infty} R_{S_1S_1}(\mathbf{r},t;\mathbf{r}',t')$$

$$\times \exp^{-i(\omega t-\omega' t')}dt\,dt'. \tag{21}$$

Assuming the excitation to be weakly stationary, the correlation function for the wall pressure will depend only on the temporal separation $t-t'$. In this case, it can be shown[18] that the correlation functions for the responses also depend only on the temporal separation. Subsequently, the cross spectral densities depend only on a single frequency parameter. Thus for stationary excitations, Eqs. (20) and (21) may be combined to yield

$$\Phi_{S_1S_1}(\mathbf{r},\mathbf{r}',\omega) = d^2 \int\int_R d^2\mathbf{s} \int\int_{R'} d^2\mathbf{s}'\, \Phi_{pp}(\mathbf{s},\mathbf{s}',\omega)$$

$$\times H_{xx}(\mathbf{r},\mathbf{s},\omega)H^*_{x'x'}(\mathbf{r}',\mathbf{s}',\omega). \tag{22}$$

Similarly,

$$\Phi_{S_1S_2}(\mathbf{r},\mathbf{r}',\omega) = d^2 \int\int_R d^2\mathbf{s} \int\int_{R'} d^2\mathbf{s}'\, \Phi_{pp}(\mathbf{s},\mathbf{s}',\omega)$$

$$\times H_{xx}(\mathbf{r},\mathbf{s},\omega)H^*_{y'y'}(\mathbf{r}',\mathbf{s}',\omega), \tag{23}$$

where the frequency influence function $H(\mathbf{r},\mathbf{s},\omega)$ is defined as

$$H(\mathbf{r},\mathbf{s},\omega) \equiv \int_{-\infty}^{\infty} h(\mathbf{r},\mathbf{s},t)e^{-i\omega t}\,dt, \tag{24}$$

and Φ_{pp} is the Fourier transform of R_{pp} with respect to time. The subscripts on H denote partial derivatives with respect to $\mathbf{r}$ or $\mathbf{r}'$.

For spatially homogeneous excitations, Φ_{pp} will depend only on the spatial separation. In this case, we can replace the integrands of Eqs. (22) and (23) by their spatial Fourier transforms to obtain

$$\Phi_{S_1S_1}(\mathbf{r},\mathbf{r}',\omega) = d^2 \int_{-\infty}^{\infty}\int\int \Psi_{pp}(\mathbf{k},\omega)G_{xx}(\mathbf{r},\mathbf{k},\omega)$$

$$\times G^*_{x'x'}(\mathbf{r}',\mathbf{k},\omega)d^2k, \tag{25}$$

where

$$\Psi_{pp}(\mathbf{k},\omega) = \left(\frac{1}{2\pi}\right)^2 \int_{-\infty}^{\infty}\int\int \Phi_{pp}(\mathbf{s}-\mathbf{s}',\omega)e^{-i\mathbf{k}\cdot(\mathbf{s}-\mathbf{s}')}d(\mathbf{s}-\mathbf{s}')$$

and

$$G_{xx}(\mathbf{r},\mathbf{k},\omega) = \int\int_R H_{xx}(\mathbf{r},\mathbf{s},\omega)e^{i\mathbf{k}\cdot\mathbf{s}}\,d^2\mathbf{s}. \tag{26}$$

Similar expressions are obtained for $\Phi_{S_2S_2}$ and $\Phi_{S_1S_2}$. The function $G(\mathbf{r},\mathbf{k},\omega)$ is called the sensitivity function. (As before, subscripts on G and H denote partial derivatives.) This function represents the structural response at point $\mathbf{r}$ when the excitation is harmonic, having wave number $\mathbf{k}$ and frequency ω.

For linear structures, Lin,[18] Strawderman,[3] and others have shown that the sensitivity function may be written as a superposition of normal modes. Using the method of Lin we obtain

$$G_{xx}(\mathbf{r},\mathbf{k},\omega) = \begin{cases} \sum_{m=1}^{\infty} \dfrac{\partial^2 f_m(\mathbf{r})}{\partial x^2} S_m(\mathbf{k})H_m(\omega), & \text{for } \mathbf{r}\in R, \\ 0, & \text{for } \mathbf{r}\in R, \end{cases} \tag{27}$$

where $f_m(\mathbf{r})$ is the normal mode m for the plate *in vacuo*, and

$$S_m(\mathbf{k}) = \int\int_R f_m(\mathbf{r})e^{i\mathbf{k}\cdot\mathbf{r}}\,d^2r. \tag{28}$$

The factor $H_m(\omega)$ is called the frequency response function of mode m and is defined as the modal displacement of the panel when the excitation is a unit harmonic pressure having wave numbers corresponding to mode m. The function S is commonly referred to as the modal shape function.

From Eqs. (25) and (27) we obtain

$$\Phi_{S_1S_1}(\mathbf{r},\mathbf{r}',\omega) = d^2 \sum_{m,n}^{\infty} \frac{\partial^2 f_m(\mathbf{r})}{\partial x^2}\frac{\partial^2 f_n^*(\mathbf{r}')}{\partial x'^2} H_m^*(\omega)H_n(\omega)$$

$$\times \int_{-\infty}^{\infty}\int\int \Phi_{pp}(\mathbf{k},\omega)S_m(\mathbf{k})S_n^*(\mathbf{k})d^2k. \tag{29}$$

Similarly,

$$\Phi_{S_1S_2}(\mathbf{r},\mathbf{r}',\omega) = d^2 \sum_{m,n}^{\infty} \frac{\partial^2 f_m(\mathbf{r})}{\partial x^2}\frac{\partial^2 f_n^*(\mathbf{r}')}{\partial y'^2} H_m^*(\omega)H_n(\omega)$$

$$\times \int_{-\infty}^{\infty}\int\int \Phi_{pp}(\mathbf{k},\omega)S_m(\mathbf{k})S_n^*(\mathbf{k})d^2k. \tag{30}$$

Equation (29) also gives $\Phi_{S_2S_2}$ by replacing $\partial/\partial x$ with $\partial/\partial y$.

Equations (29) and (30) give the cross spectral densities for strains in terms of the modal response of the structure and the wave-number frequency spectrum of the excitation. The power spectral density for flexural noise can now be found by combining the Fourier transform of Eq. (14) with Eqs. (29) and (30). Again invoking temporal stationarity, the time Fourier transform of Eq. (14) yields

$$\Phi_{ww}(\omega)=\left(\frac{d}{Ng_h l_x l_y}\right)^2\int_{-\infty}^{\infty}\int d^2r\int_{-\infty}^{\infty}\int d^2r'\,[h_{31}^2\Phi_{S_1S_2}(\mathbf{r},\mathbf{r}',\omega)+2h_{31}h_{32}\Phi_{S_1S_2}(\mathbf{r},\mathbf{r}',\omega)+h_{32}^2\Phi_{S_2S_2}(\mathbf{r},\mathbf{r}',\omega)]A(\mathbf{r})A(\mathbf{r}'). \tag{31}$$

Combining Eqs. (29)–(31) we obtain

$$\Phi_{pp}(\omega)=\left(\frac{d}{Ng_h l_x l_y}\right)^2\sum_{m,n}H_m(\omega)H_n^*(\omega)\times\int_{-\infty}^{\infty}\int\Psi_{pp}(\mathbf{k},\omega)S_m(\mathbf{k})S_n(\mathbf{k})d^2k\times\int_{-\infty}^{\infty}\int d^2\mathbf{r}\int_{-\infty}^{\infty}\int d^2\mathbf{r}'\left(h_{31}^2\frac{\partial^2 f_m(\mathbf{r})}{\partial x^2}\frac{\partial^2 f_n(\mathbf{r}')}{\partial x'^2}+h_{32}^2\frac{\partial^2 f_m(\mathbf{r})}{\partial y^2}\frac{\partial^2 f_n(\mathbf{r}')}{\partial y'^2}\right)A(\mathbf{r})A(\mathbf{r}'). \tag{32}$$

If we define

$$\Phi_{p_{mn}}(\omega)\equiv\int_{-\infty}^{\infty}\int\Psi_{pp}(\mathbf{k},\omega)S_m(\mathbf{k})d^2k, \tag{33}$$

and

$$\alpha_{mn}(\mathbf{r},\mathbf{r}')\equiv h_{32}^2\frac{\partial^2 f_m}{\partial x^2}\frac{\partial^2 f_n}{\partial x'^2}+h_{31}h_{32}\frac{\partial^2 f_n}{\partial x'^2}\frac{\partial^2 f_m}{\partial y^2}+h_{31}h_{32}\frac{\partial^2 f_m}{\partial x^2}\frac{\partial^2 f_n}{\partial y'^2}+h_{32}^2\frac{\partial^2 f_m}{\partial y^2}\frac{\partial^2 f_n}{\partial y'^2}, \tag{34}$$

then Eq. (32) can be written as

$$\Phi_{pp}(\omega)=\left(\frac{d}{Ng_h l_x l_y}\right)^2\sum_{m,n}H_m(\omega)H_n^*(\omega)\Phi_{p_{mn}}(\omega)\times\int_{-\infty}^{\infty}\int d^2r\int_{-\infty}^{\infty}\int d^2r'\,\alpha_{mn}(\mathbf{r},\mathbf{r}')A(\mathbf{r})A(\mathbf{r}'). \tag{35}$$

Equation (35) is the central result of this paper. It provides the formal connection between the wave number-frequency spectral density of the excitation field and the power spectral density for the equivalent-plane-wave pressure sensed by the array. This relationship is the analog of Eq. (11), the formula that is used for direct path flow noise. The term $\Phi_{p_{mn}}$ in Eq. (35) is the analog of the term $P(\mathbf{k},\omega)$ in Eq. (11). It accounts for the spectrum of the excitation field through the relationship given by Eq. (33), where Ψ_{pp} is identical to $P(\mathbf{k},\omega)$. The last term in Eq. (35) is the analog of the product of the array and hydrophone functions in Eq. (11). This term depends on the size and location of the sensors in the array. The terms $H_m(\omega)$ and $H_n^*(\omega)$, called frequency response functions (FRF), are not found in Eq. (11). These terms account for the response of the plate to each modal component of pressure in the spectrum of the excitation field. The FRF depends upon the material properties of the plate as well as the effects of water loading and intermodal coupling.

The double sum over modes in Eq. (35) can be thought of as representing a type of intermodal coupling. Thus one could have two types of intermodal coupling: (1) via the water loading on the plate, and (2) via the off-diagonal terms in Eq. (35). These off-diagonal terms arise from cross correlations of normal mode strains.

IV. THE MODAL FREQUENCY RESPONSE FUNCTION

The modal frequency response function $H_m(\omega)$ can be found by solving for the steady-state motion of the system when a unit-amplitude, harmonic force is applied in mode m. For a rectangular isotropic thin plate, simply supported and fluid loaded on one side, Lin[18] derives the following frequency response function:

$$H_m(\omega)=\frac{4}{L_xL_y}\left(D(k_{m_x}^2+k_{m_y}^2)^2-\mu\omega^2-\frac{i\rho_f\omega^2}{\sqrt{k_a^2-k_{m_x}^2-k_{m_y}^2}}\right)^{-1},\quad m=(m_x,m_y), \tag{36}$$

where L_x and L_y are the plate dimensions, μ is the mass per unit area of the plate, D is the plate flexural rigidity, k_a is the acoustic wave number, and ρ_f is the density of the fluid. The modal wave numbers are given by

$$k_{m_x}=m_x\pi/L_x,\quad m_x=0,1,2,\ldots \tag{37}$$

and

$$k_{m_y}=m_y\pi/L_y,\quad m_y=0,1,2,\ldots .$$

Equation (36) provides a good model for the frequency response function if the mass and stiffness of the isotropic support plate are much greater than those of the sensors and the outer decoupler and, in addition, the fluid loading is adequately represented by the last term in this equation. When the support plate is orthotropic, and/or comparable in mass and stiffness to the other components, then the entire structure must be thought of as a composite layered plate or shell as shown in Fig. 3. In such cases, the frequency response function may be obtained using the Donnel shell theory as generalized by Dong[19] to include layered shells. If the radius of curvature of the shell is much greater than the other dimensions of the shell, then

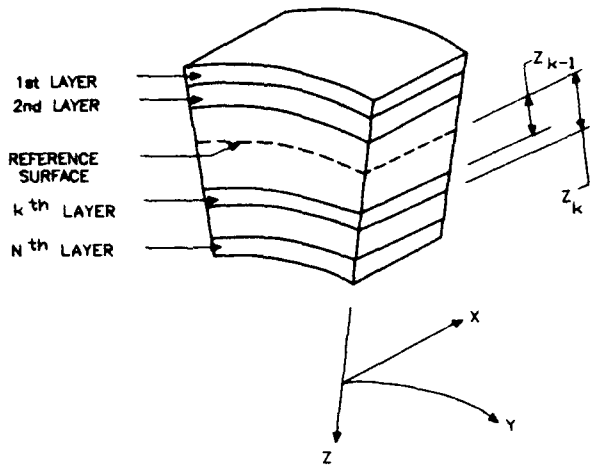

FIG. 3. Cutaway view of the array considered as a multilayered cylindrical plate.

the Donnel theory reduces to the following equations for the motion.[20]

Assuming that the plate is simply supported, the displacement can be expressed as a summation of *in vacuo* modes; i.e.,

$$w=\sum_{m_x=1}^{\infty}\sum_{m_y=1}^{\infty} w_{m_x m_y}\sin(k_{m_x}x)\sin(k_{m_y}y). \tag{38}$$

Any externally applied pressure can be similarly written as

$$q_F=\sum_{m_x=1}^{\infty}\sum_{m_y=1}^{\infty} q_{m_x m_y}\sin(k_{m_x}x)\sin(k_{m_y}y). \tag{39}$$

The generalized applied force in mode m is defined as

$$F_{m_x m_y}=\int_0^{L_y}\int_0^{L_x} q_f \sin(k_{m_x}x)\sin(k_{m_y}y)\,dx\,dy. \tag{40}$$

Using orthogonality of the *in vacuo* modes, one finds that

$$F_{m_x m_y}=(L_x L_y/4)q_{m_x m_y}. \tag{41}$$

The acoustic pressure created by the vibration of the plate can be expressed in like fashion:

$$P_a=\sum_{m_x=1}^{\infty}\sum_{m_y=1}^{\infty} P_{m_x m_y}\sin(k_{m_x}x)\sin(k_{m_y}y). \tag{42}$$

For a shallow layered shell it has been shown[20] that the Donnel theory yields the following equation of motion:

$$[D_{11}(k_{m_x}^4+k_{m_y}^4)+2(D_{12}+2D_{66})k_{m_x}^2k_{m_y}^2-\mu\omega^2]w_{m_x m_y}$$
$$=(4/L_xL_y)F_{m_x m_y}-P_{m_x m_y}, \tag{43}$$

where D_{11}, D_{12}, and D_{66} represent the flexural rigidity constants for a layered plate. These are defined[19] in terms of Young's modulus and Poisson's ratio. For a single layer of isotropic material, these equations reduce to the classical equation of motion for a thin rectangular plate.

V. WATER-LOADING EFFECT

This problem has been studied by many authors.[22–26] Most of the available models have been summarized by Leibowitz.[27] The major complication arising from water loading is that the orthogonal *in vacuo* eigenmodes become intercoupled by the water loading. That is, the interaction of the fluid and plate for one mode is a function of all the other modes.

We shall adopt the Junger and Feit model as described by Leibowitz;[27] this model was developed for symmetric modes of the plate. However, the analytical result is valid for both symmetric and antisymmetric modes (Leibowitz,[27] Table I).

The Junger and Feit model for the water loading on mode (m,n) can be expressed as

$$P_{mn}=i\omega\sum_{pq} I_{mnpq}w_{pq}, \tag{44}$$

where

$$I_{mnpq}=\frac{\rho\omega k_m k_n(-1)^{m+n}}{\pi^2}\sum_{pq}(-1)^{p+q}k_p k_q\cdot\left(\int\int_{\infty}\frac{\cos^2\gamma_x L_x\cos^2\gamma_y L_y\,d\gamma_x\,d\gamma_y}{(k^2-\gamma_x^2-\gamma_y^2)^{1/2}(k_m^2-\gamma_x^2)(k_n^2-\gamma_y^2)(k_p^2-\gamma_x^2)(k_q^2-\gamma_y^2)}\right)$$
$$=(r_{mnpq}-i\omega m_{mnpq})L_xL_y, \tag{45}$$

where

$$r_{mnpq}=\mathrm{Re}(I_{mnpq}/L_xL_y), \tag{46}$$

$$m_{mnpq}=-(1/\omega)\mathrm{Im}(I_{mnpq}/L_xL_y). \tag{47}$$

By examining Eq. (44) we see that each mode (m,n) is coupled to all of the other modes via the term I_{mnpq}.

Leibowitz[27] has shown that the cross-coupling terms are much smaller than the self-impedance components when k_aL_x and $k_aL_y>3$, which are equivalent to $k_{m_x}L_x$ and $k_{m_y}L_y\gg 1$ (the thin plate criteria) provided that $\omega\ll\omega_c$. Here k_a is the acoustic wave number ω/c. This criteria is satisfied for the SSP over the frequency band of interest. Moreover, Sandman[11] has shown that when moderate structural damping is included, the cross-coupling terms are negligible. For reassurance cross-coupling terms were computed numerically and were found to be negligible for the problem of interest to be discussed below.

TABLE I. Water loading: Comparison of approximate and exact methods.

I_{mngr}	Frequency = 8 kHz Approximate (Ns/m)	Exact[11] (Ns/m)
$I_{11\,11}$	1.368×10^{7}	$(1.357\times10^{7}-j1.666\times10^{6})$
$I_{20\,20\,20\,20}$	7.687×10^{7}	$(5.208\times10^{7}-j2.671\times10^{7})$
$I_{21\,21\,21\,21}$	$j5.222\times10^{7}$	$(2.160\times10^{7}+j4.963\times10^{7})$
$I_{30\,30\,30\,30}$	$j1.253\times10^{7}$	$(3.281\times10^{7}+j1.162\times10^{7})$

VI. APPROXIMATE WATER LOADING

When cross terms are negligible the Junger and Feit model[10] for the acoustic pressure can be written as

$$P_{m_x m_y}\approx\frac{i\rho_f\omega^2 w_{m_x m_y}}{\sqrt{k_a^2-k_{m_x}^2-k_{m_y}^2}}, \tag{48}$$

where ρ_f is the density of water and k_a is the acoustic wave number.

As a check on the Junger and Feit approximation, some typical modes were computed and the results compared to the more exact results of Sandman.[11] The specific example considered consisted of a 0.0254-m-thick cylindrical steel shell overlaid with a 0.0508-m-thick elastomer blanket. The lateral dimensions of the shell were $L_x=4$ m and $L_y=2$ m. The radius of curvature of the shell was 5.2 m. The frequency range of interest was 1 to 10 kHz. The values used for Young's modulus, Poisson ratio, and density are as follows:

Elastomer layer

$$E=1.0\times10^{6}\ \text{Pa}\quad \nu=0.49\quad \rho=1200\ \text{kg/m}^3;$$

Steel support

$$E=2.1\times10^{11}\ \text{Pa}\quad \nu=0.3\quad \rho=7900\ \text{kg/m}^3.$$

The area density μ can be found by taking the product of ρ and h. The resulting impedance values are shown in Table I for 8 kHz. The differences between the approximate values and the exact values are found to lead to errors of no more than 1 dB in the final result.

The modal displacement as computed with the radiation impedance from Sandman's[11] numerical technique was compared to a similar result using Junger and Feit's[10] approximate formula, Eq. (48). Figures 4 and 5 compare the results of these two methods for two representative sections through the plate, one parallel to the x axis, the other parallel to the y axis. The two methods give essentially the same results; i.e., the differences are less than the resolution of the plots. These results support the use of the simpler Junger and Feit expression for the purposes of modeling the TBL excitation of the SSP. The additional developments that follow will assume the Junger and Feit model is being employed; however, these developments could be generalized in a straightforward way to include Sandman's model for the water loading. Modal coupling, should it be important, could also be accommodated, but the numerical computations would become much more difficult.

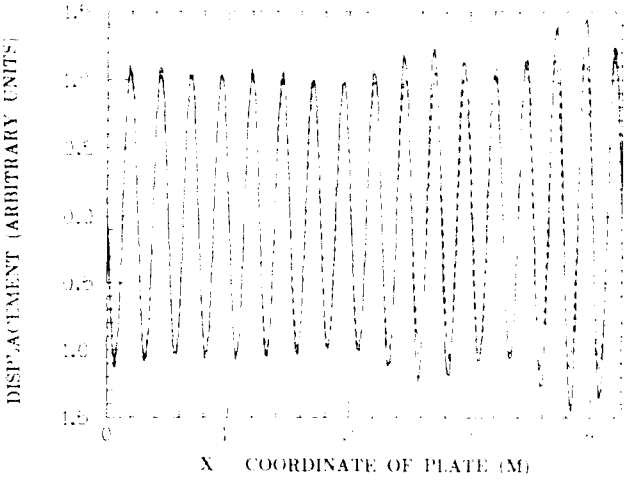

FIG. 4. A comparison of the plate displacement along the x axis obtained using the Junger and Feit[10] approximation with the displacement obtained using Sandman's "method" for obtaining water loading.

Recall from the structure of Eq. (35) that the double summation over modes introduces an additional type of modal coupling that arises from cross correlations between modes. Thus one could have two types of modal coupling: (1) via the water loading on the plate, and (2) via the *double summation in* Eq. (35). We have argued above that the first kind of modal coupling is negligible for our problem. We shall see that the second kind is also negligible.

Having established the credibility of the Junger and Feit model for water loading, we are now in a position to compute the frequency response function. Setting $F_{m_x m_y}=1$, and using Eq. (48) for the water loading, we find from Eq. (43)

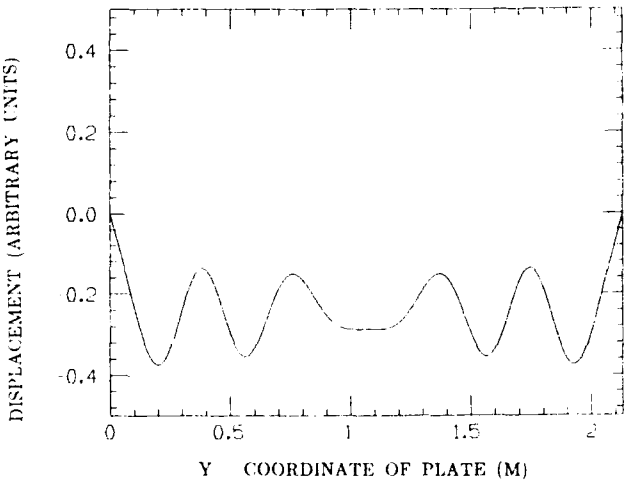

FIG. 5. A comparison of the plate displacement along the y axis obtained using the Junger and Feit[10] approximation with the displacement obtained using Sandman's "method" for the water loading.

$$H_m(\omega)=\left(D_{11}(k_{m_x}^4+k_{m_y}^4)+2(D_{12}+2D_{66})k_{m_x}^2k_{m_y}^2 - \mu\omega^2-\frac{i\rho_f\omega^2}{\sqrt{k_a^2-k_{m_x}^2-k_{m_y}^2}}\right)^{-1}\frac{4}{L_xL_y}. \quad (49)$$

VII. THE ARRAY FILTER FUNCTION

The *in vacuo* eigenfunctions for a plate of dimension L_x and L_y are

$$f_m(\mathbf{r})=\sin(k_{m_x}x)\sin(k_{m_y}y), \quad (50)$$

where m represents a pair of modal indices (m_x,m_y) that take on integral values from 1 to ∞. From Eq. (34) we have

$$\begin{aligned}\alpha_{mn}(\mathbf{r},\mathbf{r}')&=[h_{31}^2k_{m_x}^2k_{n_x}^2+h_{31}h_{32}(k_{m_x}^2k_{n_y}^2+k_{m_y}^2k_{n_x}^2)\\&\quad+h_{32}^2k_{m_y}^2k_{n_y}^2]f_m(\mathbf{r})f_n(\mathbf{r}')\\&=(h_{31}k_{m_x}^2+h_{32}k_{m_y}^2)(h_{31}k_{n_x}^2+h_{32}k_{n_y}^2)\\&\quad\times f_m(\mathbf{r})f_n(\mathbf{r}'). \quad (51)\end{aligned}$$

Integration over a single sensor located in region $R_i\in(x_i,y_i;x_i',y_i')$ yields

$$\begin{aligned}&\iint_{R_i}d^2r\iint_{R_i}d^2r'\,\alpha_{mn}\\&=(h_{31}k_{m_x}^2+h_{32}k_{m_y}^2)(h_{31}k_{n_x}^2+h_{32}k_{n_y}^2)\\&\quad\times\left(\frac{\cos k_{m_x}x_i'-\cos k_{m_x}x_i}{k_{m_x}}\right)\left(\frac{\cos k_{m_y}y_i'-\cos k_{m_y}y_i}{k_{m_y}}\right)\\&\quad\times\left(\frac{\cos k_{n_x}x_i'-\cos k_{n_x}x_i}{k_{n_x}}\right)\left(\frac{\cos k_{n_y}y_i'\quad\cos k_{n_y}y_i}{k_{n_y}}\right).\end{aligned} \quad (52)$$

The total array filter function is obtained by summing over all regions R_i occupied by the sensors.

VIII. THE MODAL SPECTRAL DENSITY OF THE EXCITATION

Before evaluating $\Phi_{p_{mn}}(\omega)$ it will first be necessary to evaluate the form factors $S_m(\mathbf{k})$, which are Fourier transforms of the mode shapes; i.e.,

$$S_m(\mathbf{k})\equiv\iint_{A_p}e^{-i\mathbf{k}\cdot\mathbf{r}}\sin(k_{m_x}x)\sin(k_{m_y}y)dx\,dy, \quad (53)$$

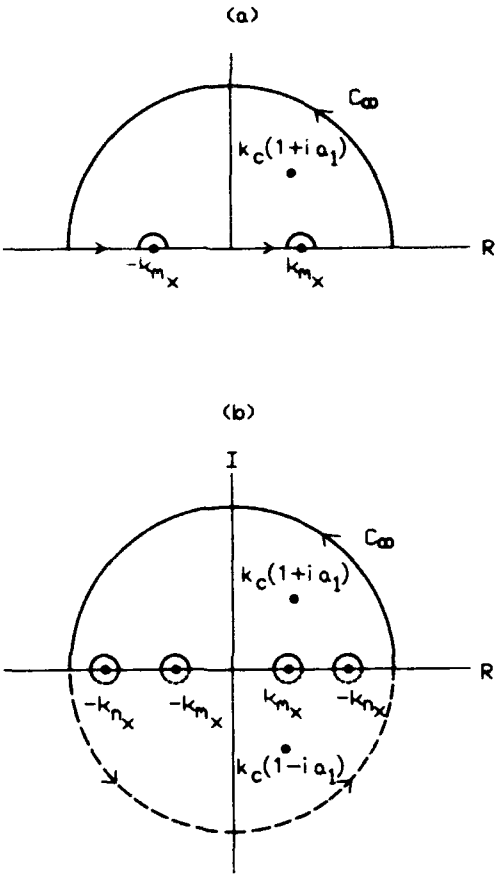

FIG. 6. Contours in the complex plane used to evaluate the modal spectral density of the turbulent boundary layer pressure field. Contour (a) is used for the diagonal terms whereas contour (b) is appropriate for the off-diagonal terms.

where A_p denotes integration over the surface of the composite SSP. This integration can easily be done by parts, yielding

$$\begin{aligned}S_m(\mathbf{k})&=\frac{k_{m_x}\{1-\exp[-i(k_xL_x-m_x\pi)]\}}{k_{m_x}^2-k_x^2}\\&\quad\times\frac{k_{m_y}\{1-\exp[-i(k_yL_y-m_y\pi)]\}}{k_{m_y}^2-k_y^2}.\end{aligned} \quad (54)$$

The power spectral density of the excitation $\Phi_{pp}(\mathbf{k},\omega)$ will be taken as the wave-number-frequency spectrum resulting from the Fourier transform of the wall pressure spectral model proposed by Corcos.[9] Following Ko and Schloemer,[17] this model can be expressed as

$$\phi_{pp}(\mathbf{k},\omega)=\frac{P(0,\omega)(\alpha_1\alpha_2k_c^2)}{\{\pi^2[(k_x-k_c)^2+(\alpha_1k_c)^2][k_y^2+(\alpha_2k_c)^2]\}}, \quad (55)$$

where $k_c\equiv\omega/U_c$ and U_c is the convection velocity.

Then $P(0,\omega)\equiv a_+(1+\gamma)\rho_f^2V_*^4/\omega$, where ρ_f is the water density and V_* is the friction velocity. The terms a_+, γ, α_1, and α_2 are empirically determined constants.

We shall first evaluate the diagonal terms of $\Phi_{p_{mn}}(\omega)(m=n)$. In this case we can combine Eqs. (33), (54), and (55) to obtain

$$\Phi_{p_{mm}}(\omega)=\phi_{p_{m_x}}(\omega)\phi_{p_{m_y}}(\omega)\beta(k_c), \tag{56}$$

where

$$\phi_{p_{m_x}}(\omega)\equiv 2\int_{-\infty}^{\infty}\frac{k_{m_x}^2[1-\cos(k_xL_x-m_x\pi)]dk_x}{(k_x^2-k_{m_x}^2)^2[(k_x-k_c)^2+(\alpha_1k_c)^2]}, \tag{57}$$

$$\phi_{p_{m_y}}(\omega)\equiv 2\int_{-\infty}^{\infty}\frac{k_{m_y}^2[1-\cos(k_yL_y-m_y\pi)]dk_y}{(k_y^2-k_{m_y}^2)^2[k_y^2+(\alpha_2k_c)^2]}, \tag{58}$$

and

$$\beta(k_c)\equiv P(0,\omega)\alpha_1\alpha_2k_c^2/\pi^2. \tag{59}$$

Consider Eq. (57). This integral can be written as

$$\phi_{p_{m_x}}(\omega)=\mathrm{Re}\left(2\int_{-\infty}^{\infty}\frac{k_{m_x}^2[1-e^{i(ZL_x-m_x\pi)}]dZ}{(Z-k_{m_x})^2(Z+k_{m_x})^2[Z-k_c(1+i\alpha_1)][Z-k_c(1-i\alpha_1)]}\right), \tag{60}$$

where the variable of the integration has been replaced by the complex number Z. This integral may be evaluated using the contour shown in Fig. 6(a). The numerator has been replaced by the real part of an exponential in order to avoid a pole where the C_∞ contour intersects the imaginary axis. There are simple poles at $-k_{m_x}$ and $+k_{m_x}$, and a second-order pole at $Z=k_c(1+i\alpha_1)$. Using the theorem of residues we find the following results:

$$\phi_{p_{m_x}}(\omega)=\mathrm{Re}\left(2\pi k_{m_x}^2\frac{1-\exp i[k_cL_x(1+i\alpha_1)-m_x\pi]}{\alpha_1k_c[k_c^2(1+i\alpha_1)^2-k_{m_x}^2]^2}\right)+\frac{\pi L_x}{2}\left(\frac{1}{(k_{m_x}+k_c)^2+(\alpha_1k_c)^2}+\frac{1}{(k_{m_x}-k_c)^2+(\alpha_1k_c)^2}\right). \tag{61}$$

The expression for $\phi_{p_{m_y}}(\omega)$ can be evaluated in a similar fashion, the only difference being that the second-order pole will be located on the imaginary axis. The result is

$$\phi_{p_{m_y}}(\omega)=2\pi k_{m_y}^2\frac{1-\exp(-\alpha_2k_cL_y)\cos m_y\pi}{\alpha_2k_c(\alpha_2^2k_c^2+k_{m_y}^2)^2}+\frac{\pi L_y}{[k_{m_y}^2+(\alpha_2k_c)^2]}. \tag{62}$$

An analogous expression for the off-diagonal terms $(m\neq n)$ is

$$\phi_{p_{mn}}(\omega)=\phi_{p_{m_x}}(\omega)\phi_{p_{m_y}}(\omega)\beta(k_c), \tag{63}$$

where

$$\phi_{p_{m_x}}\equiv k_{m_x}k_{n_x}\times\int_{-\infty}^{\infty}\frac{[1-e^{-i(k_xL_x-m_x\pi)}][1-e^{i(k_xL_x-n_x\pi)}]dk_x}{(k_x^2-k_{m_x}^2)(k_x^2-k_{n_x}^2)[(k_x-k_c)^2+(\alpha_1k_c)^2]} \tag{64}$$

and

$$\phi_{p_{m_y}}\equiv k_{m_y}k_{n_y}\times\int_{-\infty}^{\infty}\frac{[1-e^{i(k_yL_y-m_y\pi)}][1-e^{i(k_yL_y-n_y\pi)}]dk_y}{(k_y^2-k_{m_y}^2)(k_y^2-k_{n_y}^2)[k_y^2+(\alpha_2k_c)^2]}. \tag{65}$$

These are similar to the previous expressions except that there are now four simple poles on the real axis [see Fig. 6(b)] and the off-axis poles are now simple poles. The evaluation is straightforward if one writes the numerator as $1+e^{i(m_x-n_x)\pi}-e^{i(k_xL_x-n_x\pi)}-e^{-i(k_xL_x-m_x\pi)}$. The first three terms may be integrated using the upper contour in Fig. 6(b), whereas the fourth term may be integrated using the lower contour. The results will not be presented because they are at least two orders of magnitude smaller than the diagonal terms for the illustrative application discussed below. This is to be expected, for upon examination of Eq. (33) it is seen that when $\Psi_{pp}(\mathbf{k},\omega)$ is a slowly varying function in comparison to S_m and S_n, then the contributions from the orthogonal form factors S_m and S_n^* tend to cancel upon integration. Thus the cross terms are negligible except when L_x and L_y are so small that S_m and S_n vary as slowly as $\Psi_{pp}(\mathbf{k},\omega)$. Even if this were not the case, the off-diagonal terms in the array filter function are small for the problem of interest. A numerical study of the off-diagonal terms indicates that they are typically eight orders of magnitude smaller than the diagonal terms. The largest contributions from off the diagonal are terms for which three of the indices m_x, m_y, n_x, and n_y are equal, and the fourth index is only slightly different from the others. In such cases, the off-diagonal contribution is at least two orders of magnitude smaller than the diagonal terms.

Now consider the product $H_m(\omega)H_n^*(\omega)$. The diagonal terms have peaks at frequencies wher the real part of the FRF goes to zero. Figure 7 shows some examples for the case of light damping. At the FRF resonance frequencies the major contribution to the modal sum comes from only one mode. In the case of heavy damping the Q of these

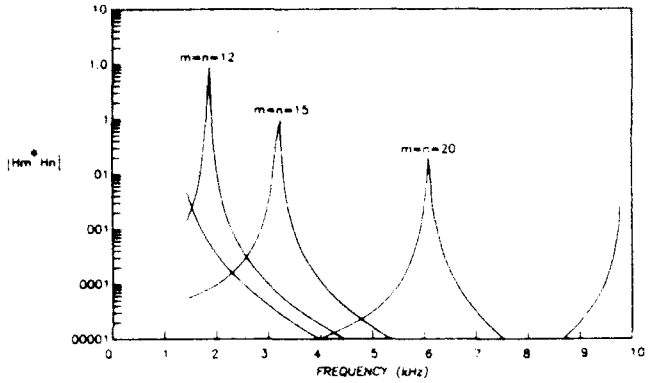

FIG. 7. An illustration of the diagonal frequency response function for a lightly damped support plate.

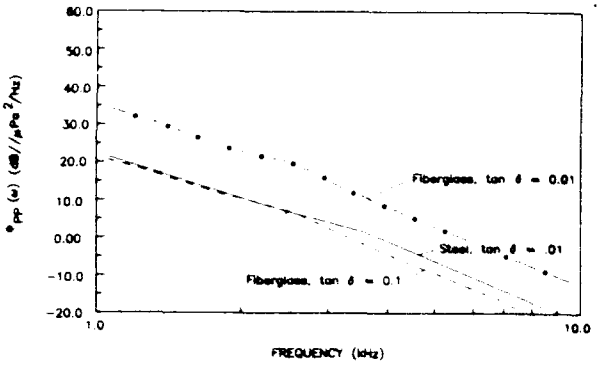

FIG. 9. The flexural noise spectral density as a function of frequency for the illustrative application discussed in the text. Results for two types of materials and loss factors are shown. The loss factors pertain to the Young's and shear moduli of the SSP.

resonances is greatly reduced; thus more than one mode may contribute. Even so, the number of modes that need to be retained is not large because only nearest neighbors contribute at that frequency. For example, as seen in Fig 7, it is evident that to compute $\Phi_{pp}(\omega)$ at about 1.25 kHz one needs only to retain modes that have indices clustered about mode $m_x=m_y=n_x=n_y=12$. Exclusion of the other modes greatly reduces the computational complexity of Eq. (33).

A representative plot of off-diagonal terms $H_m(\omega)H_n^*(\omega)$ is presented in Fig. 8. It is seen that the off-diagonal terms may have peaks at an FRF resonance frequency, but the amplitudes of the off-diagonal terms are still at least an order of magnitude smaller than the diagonal terms.

IX. NUMERICAL PROCEDURES

Because the largest values of the product $H_m(\omega)H_n^*(\omega)$ occur at the resonances of the FRF, an upper bound on $Q(\omega)$ can be found by evaluating Eq. (35) at those frequencies alone. Only a few modes about each resonance need to be retained in the summation. Additionally, the off-diagonal contributions of each term in Eq. (35) are at least two orders of magnitude less than the diagonal terms. Therefore, the product

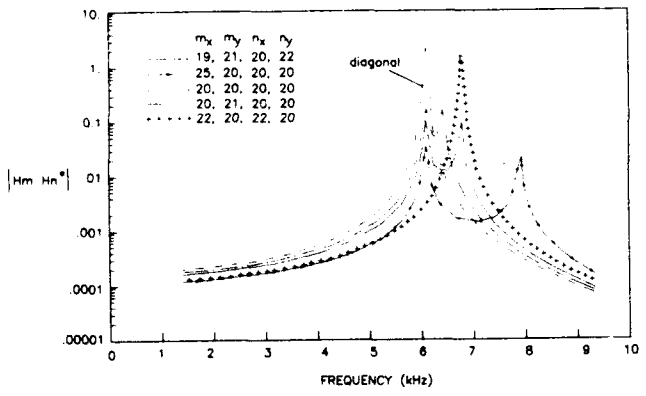

FIG. 8. An illustration of off-diagonal frequency response function for a lightly damped support plate.

$$H_m(\omega)H_n^*(\omega)\Phi_{p_{mn}}(\omega)\iint a_{mn}dx\,dy$$

is at least six orders of magnitude less for $m\neq n$ than for $m=n$. Therefore, no off-diagonal terms need to be retained.

The following procedur was used to evaluate Eq. (33). First, the resonances of the FRF in the frequency range of interest were determined. For the cases studied there are about 20 such resonances. Then, $\Phi_{pp}(\omega)$ was computed for each of these resonant frequencies by summing 100 of the nearest neighbor diagonal terms.

X. AN ILLUSTRATIVE EXAMPLE

As indicated previously, the spectral density $\Phi_{pp}(\omega)$ represents the equivalent-plane-wave pressure sensed by the array. In this form $Q(\omega)$ can be directly compared to ambient sea noise. Three specific cases have been studied numerically. All three cases are dual layer laminations consisting of an SSP and an elastomer overlayer of thickness of 0.051 m (the OD). The array consisted of 28×14 piezorubber sensors. The sensor dimensions were $0.095\times0.095\times0.0032$ m. The SSP dimensions were $L_x=3.000$ m, $L_y=2.30$ m, thickness$=0.0254$ m. The values of the empirical constants α_1, α_2, α_+, and γ, that enter Eq. (55) are a matter of some controversy in the literature. For our example, we shall use the values suggested by Ko and Schloemer,[17] Eq. (9). Thus we take,

$$\alpha_1=0.09,\quad \alpha_2=7\alpha_1,\quad \alpha_+=0.766,\quad \gamma=0.389. \tag{66}$$

The friction velocity V_* has also been evaluated using the following relationships suggested by Ko and Schloemer;

$$V_*=\sqrt{c_f/2}U, \tag{67}$$

where U is the platform speed, and c_f, the friction coefficient, is related to the Reynolds number R_x as,

$$c_f=0.455(\log R_x)^{-2.58}. \tag{68}$$

Figure 9 shows the results for a 0.0254 m SSP made of either steel or glass fiber. The platform speed is 20 kn. Two values of loss tangent were used for the glass fiber SSP to

show the influence of damping. The smaller value is more representative of practical materials.

XI. CONCLUSION

The model presented above accounts for a heretofore neglected flexural noise mechanism; i.e., direct coupling of the flexure with the lateral displacement of a planar sensor. The model was developed for piezoelectric sensors such as rubber–lead titanate composites and PVDF; however, the development could be adapted to other sensor types such as fiber optic sensors.

An exact analytical expression for the spectral density of flexural noise was derived for the case where the random excitation field is characterized by the modified Corcos model. In general, this expression involves four summations, each to infinity, over the normal modes of the plate. However, it was shown that only a few modes need to be included for each frequency of interest. Therefore, the equation for the spectral density is tractable for practical applications.

The results indicate that a 0.0254-m steel SSP of light damping and a 0.191-m glass fiber SSP of heavy damping will both perform satisfactorily. However, the result for the glass fiber SSP with light damping is comparable to direct flow noise levels. It is also seen that flexural noise increases inversely with frequency at about the same rate as sea noise. Therefore, flexural noise arising from TBL excitations could be important at lower frequencies.

The model, as applied to the example, did not account for the mechanical properties of the sensor nor for the effects of the inner decoupler. The added stiffness, mass, and damping contributed by the sensor and the ID will lower the predicted noise levels. Therefore, the results represent upper limits on flexural noise for the various types of SSPs. Inclusion of the sensor in the analysis is a straightforward process. However, to include the ID, more analytical development will be required.

The dependence of the spectral density on the array design parameters can be inferred from Eqs. (35), (49), and (52) without actually performing numerical computations. To minimize flexural noise one should do the following,

(i) Minimize d, the distance from the midplane of the SSP to the midplane of the sensor.

(ii) Maximize g_h/h_{12} and g_h/h_{13}, the ratios of the hydrostatic sensitivity to the lateral sensitivities.

(iii) Maximize the number of sensors in the array and the lateral dimensions of the SSP.

(iv) Minimize the gap between sensors. We see from Eq. (52) that if the gaps were closed in at least one dimension, then there would be essentially no noise due to flexure of the sensors. However, there still would be noise radiated into the water by the edges of the SSP.

(v) Locate the neutral axis of the flexure at the midplane of the sensor. For example, the piezorubber or PVDF type sensors could be mounted on both sides of the SSP. Then, their flexural responses would cancel. However, such a configuration would permit higher levels of other noise sources.

The limiting assumptions of the model could be addressed without modifying the basic approach. For example, the condition of a pressure-release backing to the support plate could be replaced by a specific impedance boundary condition which might represent an inner decoupler placed between the support plate and the hull of the ship. Another limiting assumption is that the structure behaves as a thin plate. This assumption manifests itself in the model via the relationships between lateral strains and the normal displacement Eq. (2). This limitation may be removed by replacing Eq. (2) with a more exact expression obtained from thick plate theory.

In conclusion, an analytical approach and a mathematical model has been developed for the case of TBL noise induced via the coupling of the lateral sensitivity of an extended sensor to the flexural vibration of the support plate. This model provides a means for computing the noise spectral density in terms of the equivalent-plane-wave pressure, and thus provides a direct comparison with ambient sea state noise levels.

ACKNOWLEDGMENT

The authors wish to express their appreciation to David Chase, Chase Inc., Boston, MA, for his review and critique of the theoretical developments.

[1] J. E. Cole, "Array noise from vibration of the signal conditioning plate," Cambridge Acoust. Associates, Inc., TM/U-1495-362 Task 3.3 (28 April 1987).
[2] W. A. Strawderman, "Turbulence-induced plate vibration: An evaluation of finite- and infinite-plate models," J. Acoust. Soc. Am. **46**, Pt. 2, 1294–1307 (1969).
[3] W. A. Strawderman and R. A. Christman, "Turbulence-induced plate vibrations: Some effects of fluid loading on finite and infinite plates," J. Acoust. Soc. Am. **52**, Pt. 2, 1538–1552 (1972).
[4] R. A. Christman, "Pressure radiated by turbulence-excited finite and infinite water-loaded plates," Naval Underwater Systems Center, New London, CT, TR4573 (4 Oct. 1973).
[5] K. L. Chandiramani, "Vibration response of fluid-loaded structures to low-speed flow noise," J. Acoust. Soc. Am. **61**, 1460–1470 (1977).
[6] K. L. Chandiramani, "Response of underwater structures to convection component of flow," J. Acoust. Soc. Am. **73**, 835–839 (1983).
[7] D. Chase, "Some model results in classical hydrodynamics," Chase Inc., Boston, MA, TM No. 51 (18 Dec. 1986).
[8] Y. B. Semenenko, "Sound radiation from a thin semi-infinite plate driven by a turbulent boundary layer," Sov. Phys. Acoust. **36**(6), 601–604 (Nov–Dec 1990).
[9] G. M. Corcos, "The structure of the turbulent pressure field in boundary layer flows," J. Fluid Mech. **18**, 353–378 (1964).
[10] M. C. Junger and D. Feit, *Sound, Structures and Their Interactions* (MIT, Cambridge, MA, 1972), 2nd ed., Chap. 8.
[11] B. E. Sandman, "Motion of a three layered elastic-viscoelastic plate under fluid loading," J. Acoust. Soc. Am. **57**, 1097–1107 (1975).
[12] D. Ricketts, "Transverse vibrations of composite piezoelectric polymer plates," J. Acoust. Soc. Am. **77**, 1097–1107 (1985).
[13] W. P. Mason, "Use of piezoelectric crystals and mechanical resonators in filters and oscillators," in *Physical Acoustics*, edited by W. P. Mason (Academic, New York, 1904), Vol. 1, Pt. A, Chap. 5.
[14] W. K. Blake, *Mechanics of Flow-Induced Sound and Vibration* (Academic, Orlando, FL, 1986), 1st ed., Vol. II, pp. 562–569.
[15] D. M. Chase and R. Stern, "Turbulent-boundary-layer transmitted into and elastic layer," Bolt Beranek and Newman Inc., Cambridge, MA, BBN TM 382 (1977).
[16] P. H. White, "Effect of transducer size, shape and surface sensitivity on the measurement of boundary-layer pressures," J. Acoust. Soc. Am. **41**, 1358–1363 (1967).
[17] S. H. Ko and H. H. Schloemer, "Calculations of turbulent boundary

layer pressure fluctuations transmitted into a viscoelastic layer," J. Acoust. Soc. Am. **85**, 1469–1477 (1989).
[18] Y. K. Lin, *Probalistic Theory of Structural Dynamics* (Krieger, Huntington, NY, 1976), Chap. 7.
[19] S. B. Dong, "Free vibration of laminated orthotropic cylindrical shells," J. Acoust. Soc. Am. **44**, 1628–1635 (1968).
[20] R. E. Montgomery, "An analytical model for turbulence induced flexural noise in large conformal sonar arrays," Naval Res. Lab., Washington, DC, NRL Memo Rep. 7175 (15 January 1993).
[21] A. Harari and B. E. Sandman, "Radiation and vibrational properties of submerged stiffened cylindrical shells," J. Acoust. Soc. Am. **88**, 1817–1830 (1990).
[22] G. Maidanik, "The influence of fluid loading on the radiation from orthotropic plates," J. Sound Vib. **3**, 288–299 (1966).
[23] R. A. Mangiarotty, "Acoustic radiation damping of vibrating structures," J. Acoust. Soc. Am. **35**, 369–377 (1963).
[24] G. Maidanik and E. M. Kerwin, "Influence of fluid loading on the radiation from infinite plates below the critical frequency," J. Acoust. Soc. Am. **40**, 1034–1038 (1966).
[25] H. G. Davies, "Sound from turbulent-boundary-layer-excited panels," J. Acoust. Soc. Am. **49**, 878–889 (1971).
[26] R. C. Leibowitz, "Methods for computing radiation damping and the vibratory response of fluid loaded and acoustically radiating finite rectangular plates subject to turbulence excitation—option 4," David Taylor Naval Ship R&D Center Report 2976D (Mar. 1972).